Sensors and Materials, Vol. 23, No. 5 (2011) 263–275
MYU Tokyo

S & M 0844

Fabrication of Gold Nanoparticle Pattern Using Combination of Self-Assembly and Two-Step Transfer

Koji Sugano*, Takashi Ozaki,
Toshiyuki Tsuchiya and Osamu Tabata

Department of Micro Engineering, Graduate School of Engineering, Kyoto University,
Yoshida-Honmachi, Sakyo-ku, Kyoto 606-8501, Japan

(Received February 17, 2010; accepted October 19, 2010)

Key words: self-assembly, gold nanoparticle, plasmonic resonance, templated-assisted self-assembly

We successfully demonstrated pattern formation of 60 nm gold nanoparticles using a highly productive combined technique of particle self-assembly and subsequent assembled particle pattern transfers. Dot and line patterns of nanoparticles were fabricated on a template substrate (SiO_2/Si) utilizing template-assisted self-assembly (TASA). The obtained dot and line patterns of nanoparticles were transferred to a flexible poly-dimethylsiloxane (PDMS) substrate (the first transfer) and were subsequently transferred onto a gold thin film fabricated on a silicon substrate (the second transfer). We defined a yield of self-assembly as a ratio of the properly assembled area to the total dot-patterned area, and investigated the dependence of the yield on the experimental conditions such as the cross-sectional profiles of the template trench pattern, the concentration of the aqueous particle dispersion, and the cleaning process. It was confirmed that the yield is mainly governed by the width of the template trench. Under optimized conditions, a self-assembly yield of 79% was obtained. The flexible PDMS substrate was used for the first transfer step of the assembled particle pattern and an average yield of 58% was achieved. The second transfer yield onto the gold thin film was 93% using surface-activation bonding between the gold surfaces of the nanoparticles and the thin film. The developed process achieved high patterning accuracy and the misalignment of the dot pattern with the interval of 300 nm was 3.2% on average.

1. Introduction

The self-assembly of nanoscale materials has attracted much attention as a building technique for nanostructure[1,2] since it enables us to utilize fascinating materials such as carbon nanotubes, quantum dots (CdSe, CdS),[3] plasmonic materials of noble metals (gold/silver sphere/rod),[4] and core/shell heterogeneous materials[5] with high productivity.

*Corresponding author: e-mail: sugano@me.kyoto-u.ac.jp

Conventional nanostructuring techniques such as electron beam lithography (EBL) and focused ion beam (FIB) are high-cost processes and have many material restrictions. Therefore, the development of a highly productive assembly method of nanomaterials is a primary requirement.

In addition, most of the characteristics of nanomaterials are enhanced and utilized effectively when nanomaterials are arranged in an accurate and appropriate order. For example, deliberately designed metal nanoparticle patterns such as gold and silver suggest novel devices such as a highly sensitive molecular sensor with surface-enhanced Raman spectroscopy (SERS)[(6)] and many nanophotonics devices[(7)] such as a plasmon waveguide. To develop these devices using the particle assembly method, it is crucial to fabricate the nanoparticle patterns that provide the most suitable properties and functions to the application, since the plasmonic resonance properties of gold and silver nanoparticles strongly depend on the particle pattern including pattern shape and number of particles.[(8)]

Here, we give an example. A line pattern of particles has been known to be suitable to achieve the large electric field enhancement at the so-called hot spot when the incident light is polarized parallel to the line pattern. The hot spot is spatially localized surface plasmonic resonance around the contact point of two particles due to a dipole interaction of particles.[(9–11)] This strong enhancement of the electric field significantly enhances the Raman signal. Furthermore, the dependence of the localized plasmonic resonance on wavelength of the incident light depends on the number of particles in the line pattern. By fabricating the line patterns of particles with the optimum number of particles, the highly sensitive SERS is expected to be realized.

Therefore, to control the plasmonc resonance properties that are suitable for a certain application, a nanoparticle patterning process with high flexibility of particle pattern is necessary in addition to the high productivity.

As our preliminary approach to address this issue, a submicron particle patterning technique of 500-nm-diameter polystyrene particles was presented.[(12)] The proposed technique is used to fabricate designed particle patterns with high accuracy by adopting template-assisted self-assembly (TASA),[(13)] as shown in Fig. 1(a). Low-cost and high-throughput mass production becomes possible by transfer of the self-assembled particle patterns by TASA and repetition of the entire process. The costly template substrate for TASA, fabricated by EBL and dry etching of silicon (Si), is reusable. Furthermore, this method enables the transfer of assembled nanoparticles onto various structures made of different materials.

In this paper, we report a pattern formation technique of one order smaller 60-nm-diameter gold nanoparticles. Gold nanoparticles are commonly used as a plasmonic material and are also expected to be applied as a material for sensing, electric nanomaterials for wiring, bump, interconnection, intermediate material for bonding, and so on. We report the effects of the cross-sectional profile of template trenches, the concentration of particle dispersion, and the cleaning process on self-assembly yield on the dot pattern. Optimizations of these parameters are required for the subsequent transfer step. Subsequently, the first and second transfer steps are optimized and demonstrated.

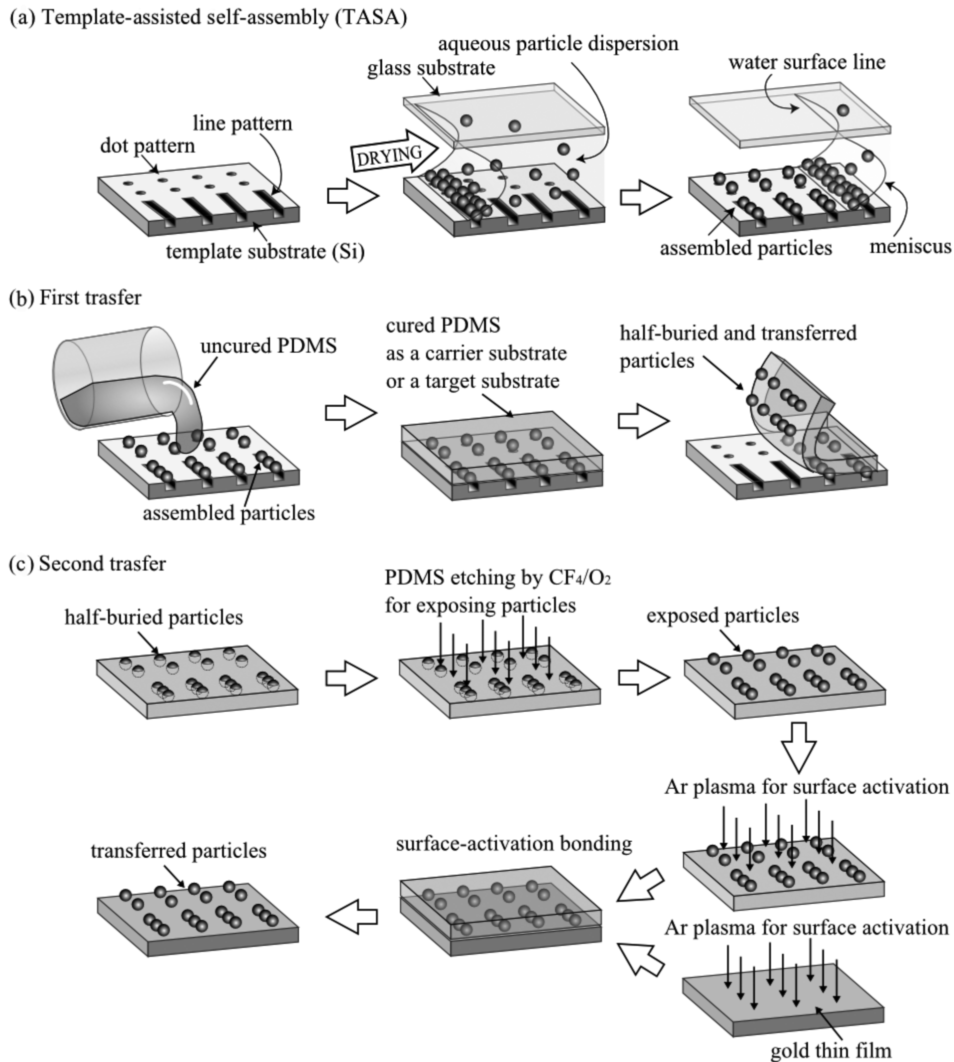

Fig. 1. Overview of the proposed process for nanoparticle pattern formation. (a) Template assisted self-assembly, (b) first transfer, and (c) second transfer.

2. Process Overview

The proposed process consists of two steps, TASA and transfer steps, as shown in Fig. 1:

1) TASA step (Fig. 1(a))

Particles are assembled onto nanoscale trenches on a template substrate (SiO_2/Si) using TASA as shown in Fig. 1(a). An aqueous particle dispersion is injected between a cover glass and a template substrate with trenches. By drying the aqueous particle

dispersion, the water surface line of the meniscus moves backward, and the particles are concentrated near the edge of the meniscus. Capillary force drags and presses the particles onto the template substrate. When the meniscus passes over the template trenches, the particles are trapped.

2) Transfer step

The self-assembled particles are transferred from the template substrate to a target substrate directly or via a carrier substrate. In this paper, direct transfer onto a flexible poly-dimethylsiloxane (PDMS) substrate and two-step transfer onto a gold thin film on a Si substrate via the PDMS carrier substrate are demonstrated.

2-1) First transfer step (Fig. 1(b))

In the first transfer step from the template substrate to the PDMS substrate as a target substrate or a carrier substrate, an uncured PDMS solution was poured onto the template substrate and then cured. The cured PDMS substrate was peeled off from the template substrate with the assembled particles.

2-2) Second transfer step (Fig. 1(c))

In the second transfer step from the carrier PDMS substrate to gold thin film, firstly, half-buried particles on the PDMS carrier substrate were exposed on the substrate by PDMS etching using CF_4 and O_2 gasses. Then, the exposed particles were transferred onto a gold thin film as a target substrate by surface-activation bonding between particles and gold thin film.

The following are features of this method.

1. High flexibility and accuracy of particle patterns are obtained at the self-assembly step.
2. Low-cost and high-throughput mass production is realized because of the high reusability of costly template substrates for self-assembly by applying the transfer steps.
3. The particle patterns are formed on various materials and on three-dimensional (3D) microstructures such as micro-electromechanical systems (MEMS) by the transfer steps.
4. Repetition of the transfer step can provide patterns of heterogeneous particles and 3D particle structures.

3. Template-Assisted Self-Assembly (TASA)

3.1 *TASA Experiment*

The template trenches of Si are fabricated by EBL and reactive ion etching (RIE) of Si. Colloidal gold particles with a mean diameter of 60 nm (British Biocell International) were used. The template substrate, which had been repeatedly used for the self-assembly, was used for the experiments in this paper and it was cleaned by the following procedure just before the experiments: 1) KI+I_2 for etching of the previously assembled and aggregated gold particles: 10 min, 2) pure water: 20 min, 3) piranha solution: 20 min, and 4) pure water: 20 min.

We investigated the effects of the cross-sectional profile of template trenches, the concentration of particle dispersion, and the cleaning process on the self-assembly yield

on the dot pattern with shallower trenches than the particle diameter, which is required for the subsequent transfer step. A template area after the assembly is divided into the following three areas: (1) where no particles exist, (2) where particles are properly assembled (properly assembled area), and (3) where excessive particles aggregate (excessively assembled area). We define the self-assembly yield as the ratio of the properly assembled area to the total dot-patterned area. The self-assembly yield was evaluated from scanning electron microscopy (SEM) images of the dot pattern.

Figure 2 shows the cross-sectional profiles of the template trenches. Four types (A–D) of cross-sectional profiles, which have different widths and depths, were fabricated. Highly selective SF_6 etching of Si to the resist was utilized to fabricate sharply edged trenches (Shapes A, B, and C). A tapered sidewall (Shape D) was fabricated using a low-selectivity gas, CF_4.

3.2 *Results and Discussion*

The effects of the cross-sectional shapes of the template trench and the concentration of aqueous particle dispersion on self-assembly yield are shown in Figs. 3 and 5, respectively.

The average self-assembly yields with Shapes A–D were about 0, 64, 65, and 96%, respectively, as shown in Fig. 3. The narrowest width trench (Shape A) showed almost no assembled particles. Shape B and Shape C, which has a deeper trench than Shape B, have no marked differences in the self-assembly yield. The widest trench (Shape D) showed the highest yield.

The characteristics of the self-assembly process on width, depth and cross-sectional profile of a template trench can be considered as follows. Width has an effect on the probability of the particles to be trapped at a template trench in which particles pass through. Depth and cross-sectional profiles have an effect on trapping force, which

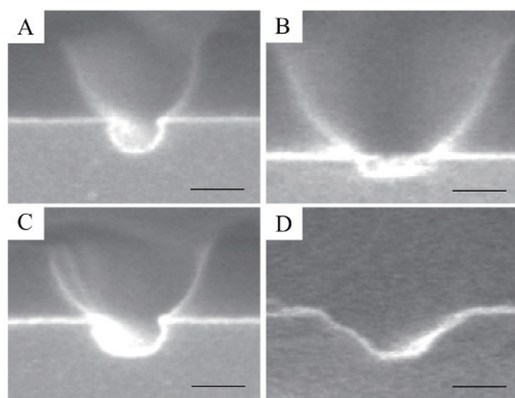

Fig. 2. SEM images of each cross-sectional profile for Shapes A–D (Shapes A–C: before resist removal). Trench width and height are (A) 40 and 40 nm, (B) 57 and 11 nm, (C) 70 and 45 nm, and (D) 150 and 44 nm, respectively. Scale bars indicate 40 nm.

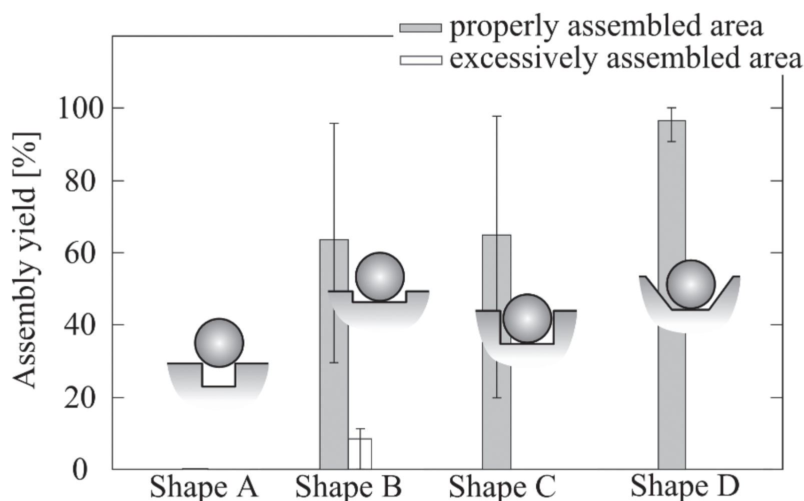

Fig. 3. Relationship between cross-sectional profile of template and yield of self-assembly. The concentration of particles was 0.0007 wt%.

attracts nanoparticles at template trenches. According to the experimental results, the trench width is a more effective parameter for the trapping of nanoparticles than the depth or cross-sectional profile. This indicates that the trench width governs the yield of TASA. Furthermore, it indicates that the shallow depth of 10 nm of Shape B and the tapered cross section of Shape D have a sufficiently large trapping force to keep a particle in a template trench.

As the second consideration, the cross-sectional profiles were evaluated from an arrangement of assembled particles in a template trench, as shown in Fig. 4. Although Shape D showed the highest self-assembly yield for a dot pattern, Shape D formed a disarranged line of particles along the line pattern. On the other hand, precisely arranged lines were formed in Shapes A–C.

From consideration of the transfer step from the template substrate to a PDMS substrate by curing the PDMS solution described in § 2, Shape B, which has shallower trenches, is preferable than Shape C to grab particles by PDMS.

Figure 5 shows the relationship between yield and concentration. Figure 6 shows atomic force microscopy (AFM) images at particle concentrations of 0.0007, 0.002, and 0.007 wt%. At a particle concentration of 0.0002 wt%, no particles were assembled and aggregated due to an excessively low concentration of particles. The particle concentration of 0.0007 wt% showed the highest assembly yield and few aggregations of particles. The assembly yield decreased with a further increase in the particle concentration from 0.0007 to 0.007 wt%.

We investigated the reason for the decrease in the assembly yield from 0.0007 to 0.007 wt% considering the morphology of aggregation on a substrate shown in Fig. 6. A one-particle-layer film was formed by the aggregation of particles inside the template area at a particle concentration of 0.002 wt%, as shown in Fig. 6(b). This is because particles

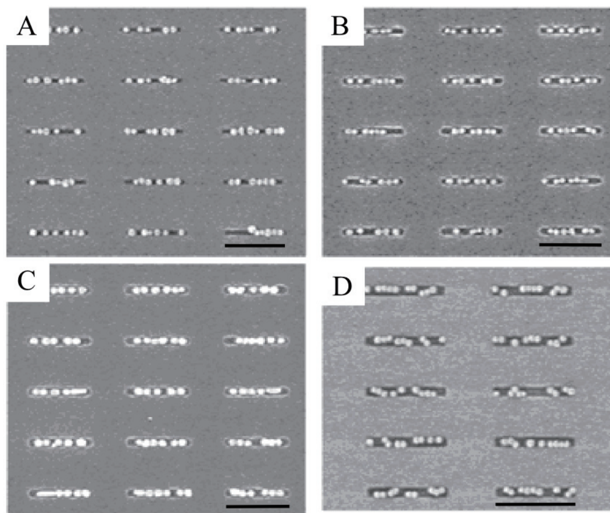

Fig. 4. Arrangement of the assembled particles on the template trenches with different cross-sectional profiles (Shapes A–D). Scale bars indicate 600 nm.

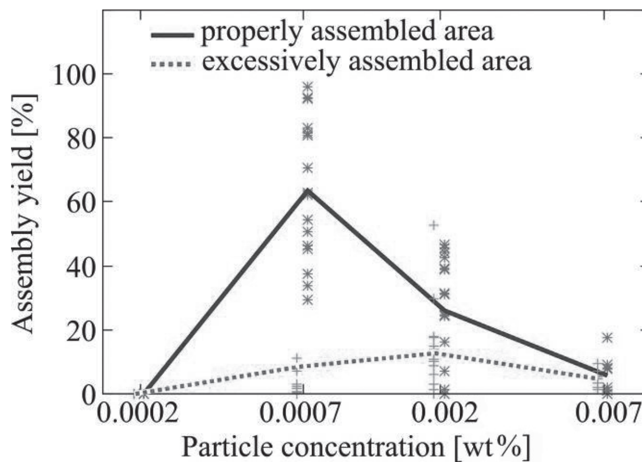

Fig. 5. Relationship between concentration of particles in dispersion and self-assembly yield. The cross-sectional profile was of Shape B.

are concentrated on the fringe of the meniscus by capillary force and then remain as a substrate, as schematically shown in Fig. 7(a). A large cluster of particles was formed by the aggregation of particles outside the template area at the particle concentration of 0.007 wt%, as shown in Fig. 6(c). The particle aggregation at the particle concentration of 0.007 wt% is considered to happen in a solution at the fringe of the meniscus and/or

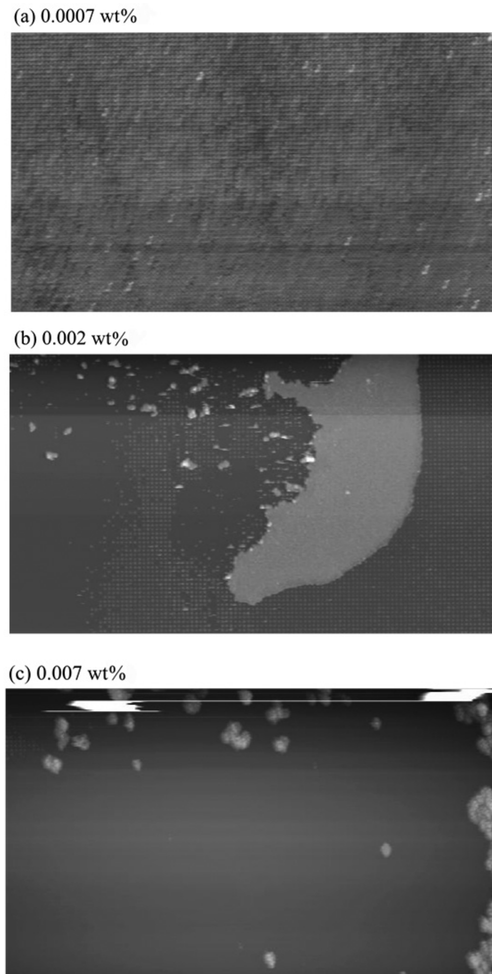

Fig. 6. AFM images of the particle-assembled template substrate at the concentrations of (a) 0.0007, (b) 0.002, and (c) 0.007 wt%.

on the substrate surface as schematically shown in Figs. 7(b-1) and 7(b-2). The reason for the decrease in assembly yield with increasing particle concentration from 0.0007 to 0.007 wt%, shown in Fig. 5, was considered to be attributed to the particle aggregation on the substrate as mentioned before. Since the increase in particle concentration induces particle aggregation, which consumes many particles, the actual net particle concentration supplied to a self-assembly area with template trenches becomes very low. Consequently, this lowering of particle concentration resulted in decreases in self-assembly yield, the same as the particle concentration of 0.0002 wt%.

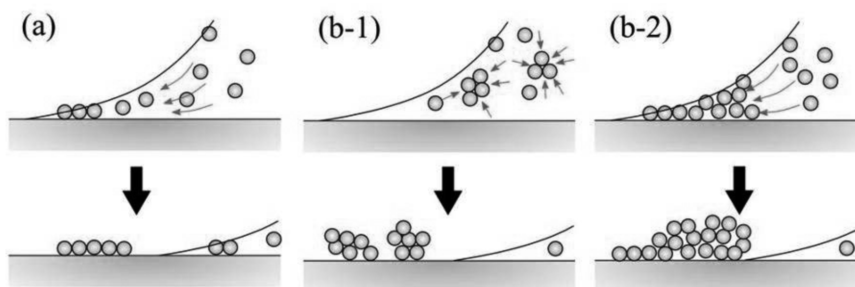

Fig. 7. Schematics of process and morphology of particle aggregation at particle concentrations of (a) 0.002 and (b) 0.007 wt%.

As the next step, the effect of the cleaning process was investigated. The increase in the etching time for the previously assembled and aggregated gold particles by $KI+I_2$ from 10 to 30 min improved the average self-assembly yield from 64 to 79% at the concentration of 0.0007 wt% with Shape B. This indicates that the remaining gold particles on the template substrate due to the insufficient gold etching cause further aggregation of particles because they pin the water surface, and particles are concentrated there by capillary force during the subsequent TASA process.

SEM images of assembled dot patterns (interval of 300 nm) and line patterns (interval of 500 nm, length of 250 nm) are shown in Fig. 8. According to Fig. 8(b), almost all lines have three particles despite space being available for four particles at each line. This is considered to be due to the effect of the negative charge of particles. The repulsive force between negatively charged particles prevents the dense alignment of particles in a line at the template pattern. Therefore, only three particles were assembled at the trench pattern even though it has enough space for four particles.

4. Transfer of Particle Arrangement

4.1 *First transfer onto PDMS substrate*

First, the template substrate was dehydrated for 2 h at 160°C in an oven since a liquid bridge between a particle and a substrate leads to a high adhesion force and prevented the particle transfer. An uncured PDMS solution, base compound:curing agent = 10:1 or 20:1, was poured onto the template substrate under vacuum of 2 Pa. After degassing from PDMS for 30 min, PDMS was cured at a temperature of 60°C for 4 h. The cured PDMS substrate was peeled off from the template substrate with the assembled particles.

Figure 9 shows the transfer yield of assembled particles for two different weight ratios between the base compound and the curing agent. The ratio of 20:1 showed a higher transfer yield of 58% than that of 10:1. This is because of the lower viscosity and higher adhesion force of the 20:1 ratio than those of the 10:1 ratio. The PDMS substrate with the patterned particles can be utilized in various flexible devices. Alternatively, this

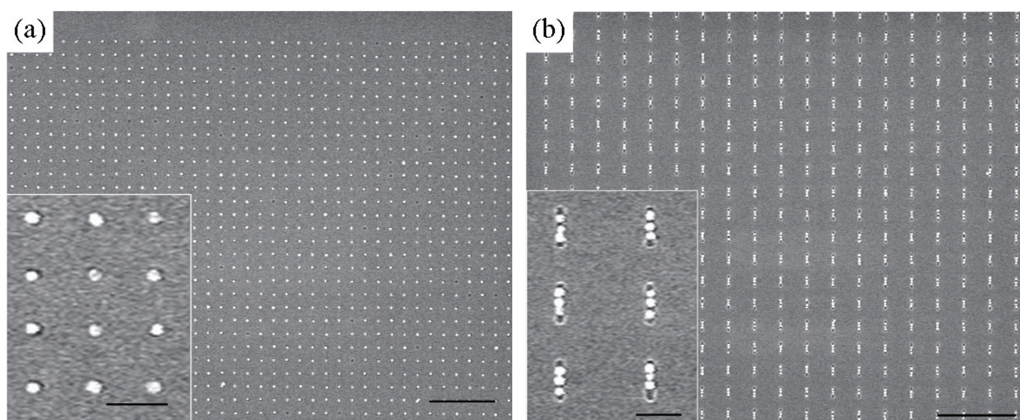

Fig. 8. Self-assembled 60 nm gold nanoparticles. Magnified figures are shown in the lower left. (a) Dot pattern (interval of 300 nm) and (b) line pattern (interval of 500 nm, length of 250 nm). Scale bars indicate 1.5 μm and 300 nm in the main images and magnified images, respectively.

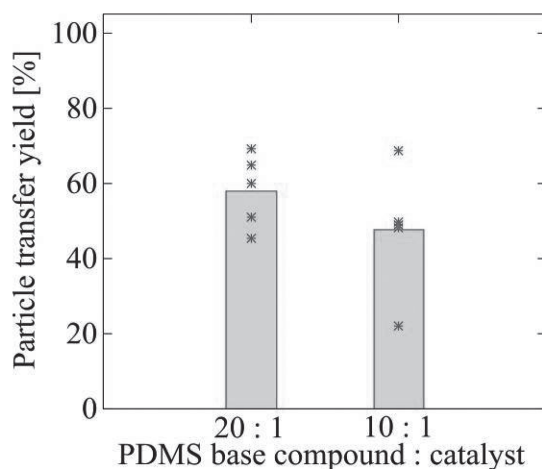

Fig. 9. Transfer yield of assembled particles depending on weight ratio between base compound and curing agent.

substrate can be used as a carrier substrate for the second transfer to target substrates of various materials.

4.2 *Second transfer onto gold thin film*

After the first transfer, the PDMS substrate was etched by RIE with a mixture of CF_4 and O_2 gases to expose the half-buried particles in the PDMS substrate. The flow rates of CF_4 and O_2 gases were 25 and 75 sccm, respectively. Gas pressure and RF

power were 6 Pa and 200 W, respectively. Figure 10 shows the exposed height of the first transferred particle as a function of etching time. The height measured by AFM increased nonlinearly with etching time. At 4 min of etching, the measured height of the exposed particle was about 39 nm. With further etching, the number of particles on the PDMS substrate markedly decreased, since the particles were completely exposed by excess etching and removed. Since the average particle height after the second transfer by the surface-activation bonding described in the next paragraph was about 40 nm, it is thought that not only the PDMS substrate but also the particles were etched by RIE. From the experiment, 2.5 min of etching was used for the second transfer onto the gold thin film to guarantee the exposed height of more than half of the particle diameter for removing particles from the PDMS substrate.

The particles on the etched PDMS substrate were successfully transferred onto a gold thin film on a Si substrate, which is a target substrate, using gold-gold surface-activation bonding. The PDMS and target substrate were irradiated by Ar plasma for 2 min at 8 W. The second transfer yield is shown in Fig. 11. A yield of 93% was achieved after 2 min

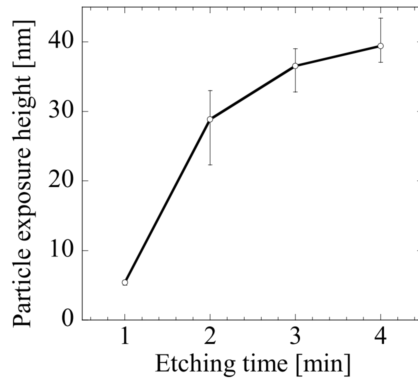

Fig. 10. Exposed height of the 1st-transferred particle as a function of etching time.

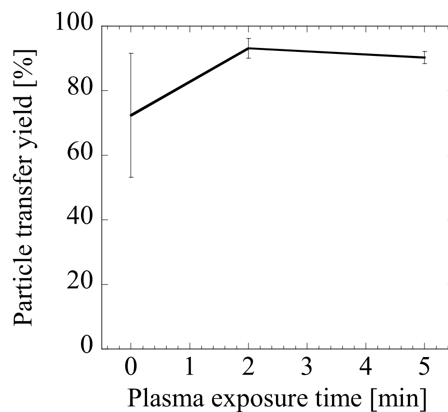

Fig. 11. Yield of the 2nd transfer as a function of irradiation time of Ar plasma.

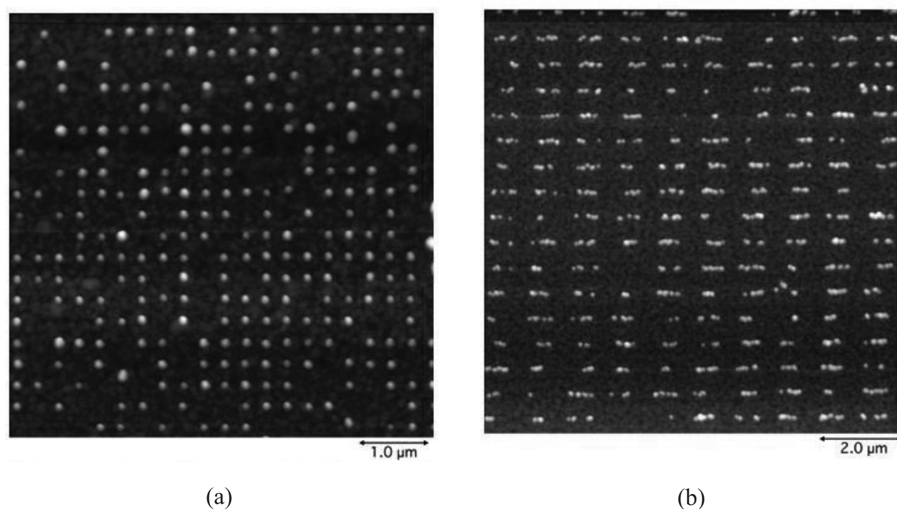

Fig. 12. AFM images of particles transferred onto gold target substrate: (a) dot pattern and (b) line pattern.

of irradiation on the dot pattern. The particle pattern was transferred onto the gold thin film, as shown in Fig. 12. According to Fig. 12, misalignment on the dot pattern with the interval of 300 nm was 3.2% on average. We successfully demonstrated the highly precise transfer of the particle patterns.

The above-mentioned methods of the first and second transfers are suitable to pattern particles very precisely since these methods provide a large adhesion force between the particles and the substrate. Depending on applications, other methods to increase the yield of the first transfer and to simplify the process without the vacuum processes of RIE and the surface activation may be necessary.

5. Conclusions

The proposed nanoparticle pattern formation method, which consists of a combination of TASA and the two-step transfer of assembled particle patterns, was successfully demonstrated using gold nanoparticles with a diameter of 60 nm.

In the self-assembly step, the effects of 1) the cross-sectional profiles of the template trench pattern, 2) the concentration of the aqueous particle dispersion, and 3) the cleaning process were investigated. According to the results, we confirmed that the self-assembly yield is mainly governed by the trapping probability of a template trench that a particle passes through. Finally, a 79% self-assembly yield was obtained on the dot pattern.

The feasibility of the subsequent particle transfer process was also demonstrated. The flexible PDMS substrate was used for the first transfer of the assembled particle pattern. The average yield of the first transfer was 58%. Subsequently, the transferred particle pattern was transferred again onto the gold thin film with a 93% transfer yield

using surface-activation bonding. Dot and line patterns of nanoparticles were fabricated on a flexible PDMS substrate and on a gold thin film.

The fabricated particle patterns using the proposed technique are expected to control plasmonic resonance effects and to be applied to highly sensitive molecular sensors with SERS and plasmonic waveguides.

Acknowledgment

This work was conducted in Kyoto-Advanced Nanotechnology Network, supported by the Ministry of Education, Culture, Sports, Science and Technology (MEXT), Japan. The authors are grateful to Sadamu Kinoshita for the SEM observations.

References

1 G. M. Whitesides and B. Grzybowski: Science **295** (2002) 2418.
2 H. Li, S. H. Park, J. H. Reif, T. H. LaBean and H. Yan: J. Am. Chem. Soc. **126** (2004) 418.
3 K. Griev, P. Mulvaney and F. Grieser: Curr. Opin. Colloid Interface Sci. **5** (2000) 168.
4 N. R. Jana, L. Gearheart and C. Murphy: J. Phys. Chem. B **105** (2001) 4065.
5 C. Graf and A. van Blaaderen: Langmuir **18** (2002) 524.
6 A. J. Haes and R. P. van Duyne: J. Am. Chem. Soc. **124** (2002) 10596.
7 S. A. Maier, M. L. Brongersm, P. G. Kik, S. Meltzer, A. A. G. Requicha and H. A. Atwater: Adv. Mater. **13** (2001) 1501.
8 M. Quinten and U. Kreibig: Surf. Sci. **172** (1986) 557.
9 L. Gunnarsson, T. Rindzevicius, J. Prikulis, B. Kasemo, M. Kll, S. Zou and G. C. Schatz: J. Phys. Chem. B **109** (2005) 1079.
10 H. Xu and M. Käll: Phys. Rev. Lett. **89** (2002) 246802.
11 Z. B. Wang, B. S. Luk'yanchuk, W. Guo, S. P. Edwardson, D. J. Whitehead, L. Li, Z. Liu and K. G. Watkins: J. Chem. Phys. **128** (2008) 094705.
12 T. Ozaki, K. Sugano, T. Tsuchiya and O. Tabata: J. Microelectromech. Syst. **16** (2007) 746.
13 Y. Yin, Y. Lu, B. Gates and Y. Xia: J. Am. Chem. Soc. **123** (2001) 8718.